Proceedings of the 2000 IEEE
International Conference on Robotics & Automation
San Francisco, CA • April 2000

On the Kinematics of Remotely-Actuated Continuum Robots

Ian A. Gravagne and Ian D. Walker
Dept. of Electrical and Computer Engineering, Clemson University, Clemson, SC
igravag@ces.clemson.edu, ianw@ces.clemson.edu

Abstract

Over the past several years, there has been a rapidly expanding interest in the the study and construction of a new class of robot manipulators which utilize high degree of freedom, or continuous, backbone structures. In this paper, we consider and illustrate some basic properties of a class of "hyper-redundant" robots, known as "continuum" robots. We base our analysis around remotely-driven, tendon-actuated manipulators such as the Rice/Clemson "Elephant's Trunk". We discuss such issues as the kinematic model, the relationship between tendon lengths and bending, and desirable design constraints for continuum robot mechanisms.

1 Introduction

By observing manipulation methods in nature, one may eventually reach the conclusion that rigid-link, low degree of freedom devices should meet the majority of manipulative and locomotive needs. However, some creatures make use of alternative methods based on very high degree of freedom (HDOF) backbones, such as snakes, or continuous "trunk" or "tentacle" structures. These manipulators, generally termed *hyper-redundant*, exhibit unique capabilities including extremely enhanced maneuverability. Hyper-redundant manipulators have the potential to navigate extremely complex paths, and to suffer localized damage or faults while still maintaining a healthy degree of functionality. In principle, this makes them suitable for a variety of delicate and dangerous tasks where a traditional robot could not reach, or where failure of a traditional robot would completely paralyze all subsequent operations. Examples of such tasks are nuclear waste inspection and removal, and navigation or inspection of highly cluttered environments such as collapsed buildings.

In this paper we will concentrate on the fundamentals of a specific type of continuum robot, frequently referring to the Rice/Clemson "Elephant's Trunk" [2]. This is a type of remotely-actuated device which uses cables, or tendons generally, to transmit forces from a motor platform into the trunk itself. The salient feature of the Elephant's Trunk is that its high number of links (16), combined with the small size of each link, allow us to closely approximate it as a truly continuous backbone. Similar to the Elephant's Trunk but much larger in scale is the GreyPilgrim "EMMA" serpentine manipulator [4]. Other robots in our laboratory do in fact possess continuous backbones made of various materials, and the following problems and theories apply to all of these robots. We will formulate a continuous backbone model for the robot kinematics, address the relationship between cable lengths for tendon-driven continuum robots, and use our observations to infer several design rules for the construction of such manipulators.

Several researchers have worked in the area of hyper-redundant or HDOF manipulators for various reasons. In Japan, Hirose pioneered the development of snake-like robots, especially with regards to locomotion; an overview of his work exists in [1]. Also, Mochiyama, et. al., have investigated the problem of controlling the shape of an HDOF rigid-link robot with two-degree-of-freedom joints using spatial curves [6]-[8]. For robots possessing continuous back-bones, known as "continuum robots", a good overview exists in [15]. These authors plus Suzumori, et. al., in [16] have done significant work in flexible hydraulic micro-actuators for grippers, which are essentially small, flexible, 3-DOF manipulators. The primary body of work upon which we draw is that of Chirikjian and Burdick, [9]-[13], who laid the foundations for the kinematic theory of hyper-redundant robots.

2 Background

Differential geometry has provided a natural starting point for the theory of hyper-redundant and continuum robots. Because we will not be using it in this paper, we defer the details of its use in robotics to other sources, including the references of Mochiyama, [6]-[8]. However, we retain the basic essence of the differential-geometric description of spatial curves; that is, a 3-dimensional curve C may be parametrically described by a vector $\underline{x}(s) \in \Re^3$, and an associated frame $Q(s) \in \Re^{3\times 3}$ whose columns create the frame bases (see figure 3), where the independent parameter s is related to the arc-length from the origin of the curve. The parameterization variable s usually varies in $s \in [0, 1]$, which is the convention in most literature. The curve is assumed continuous, and two functions, curvature $\kappa(s)$ and torsion $\tau(s)$, contain information about the shape of the curve.

Unfortunately, methods in differential geometry including the well-known "Serret-Frenet apparatus" (see [6],

[7]) do not lend themselves easily to numerical computation for various reasons. In addition, while differential-geometric methods excel at squeezing all of the descriptive information out of any particular curve, they do not in general describe actual robot kinematics without great difficulty [14].

To remedy this problem, Chirikjian and Burdick in [9]-[13] suggested a different parameterization based not upon curvature and torsion, but two "continuous angles", $K(s)$ and $T(s)$. They chose

$$Q(s) = \begin{bmatrix} c_K & s_K c_T & -s_K s_T \\ -s_K & c_K c_T & -c_K s_T \\ 0 & s_T & c_T \end{bmatrix} \quad (1)$$

with $c_K = \cos K(s)$, $s_K = \sin K(s)$,etc. The position of the robot $\underline{x}(s) = \int_0^s l(\sigma)\underline{q}_2(\sigma)d\sigma$ where $\underline{q}_2(s)$ is the second column of $Q(s)$ (the tangent to the backbone curve), and $l(s)$ is a function containing the local extensibility of the curve. Essentially, at any point s_0, (1) may be viewed as describing the frame at the end of a universal joint (U-joint) with angles $K(s_0)$ and $T(s_0)$. The robot "grows" from the origin by integrating to get $\underline{x}(s)$. At each point, $Q(s)$ contains the robot's orientation, and the robot's shape is defined by the behavior of the functions $K(s)$ and $T(s)$. In the plane, $T(s) = 0$ and $\frac{dK(s)}{ds} \equiv \kappa(s)$, the classical curvature. (For ease of notation, we say that the time-varying function $g(s,t)$ has derivatives $\frac{dg(s,t)}{ds} \triangleq \dot{g}(s)$, and $\frac{dg(s,t)}{dt}$ will be denoted explicitly or as $g_t(s,t)$ hereafter.)

While this description provides a solid foundation for a great deal of theoretical work, the specific frame $Q(s)$ illustrated in (1) still does not accurately describe the kinematics of any known physical continuum robot. Rather, it provides an "imaginary" robot to which a real (sufficiently high degree of freedom) rigid-link robot is matched or "fitted" as closely as possible. Unfortunately the method of curve fitting assumes that one can exactly control the parameters of the real robot, and that its characteristics are completely known, which is not the case in general. A continuum tendon-driven robot is essentially an infinite-degree-of-freedom device, controlled by applying forces or torques at periodic locations along the robot's backbone. Generally, this means that a specific set of tendon lengths does not imply a unique pose for the robot, so the kinematic model must reflect physical parameters such as the backbone stiffness profile, friction between the cables and the cable guides, and external forces due to gravity. These are qualities which the kinematics of traditional rigid-link robots need not reflect.

3 Kinematic Model

Although the Elephant's Trunk [2] consists of many U-joints for its backbone, their combined effect on the backbone orientation at any point does not equate to the orientation of a single U-joint, rendering the frame in (1) of limited use. The tendons exert constraints on the movement of the robot not reflected in the frame of (1) and vice versa.

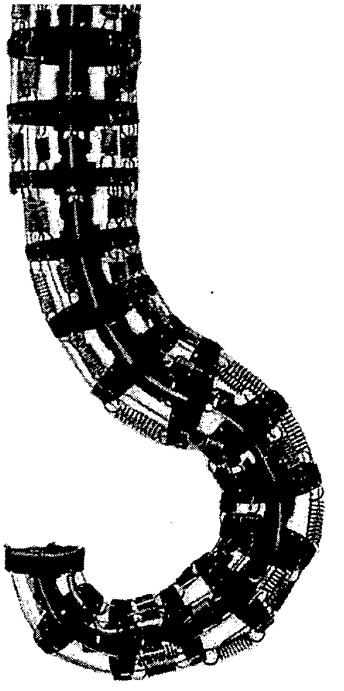

Figure 1: The Rice/Clemson Elephant's Trunk is a 4-section, 8-DOF manipulator. Its high number of links allow it to approximate continuum robots.

We begin by making some physical observations on the trunk (figure 1). It consists of 16 segments periodically spaced along the backbone, through which all the cables run. Segments keep the cable shape close to the backbone shape. Two pairs of cables attach to every 4^{th} segment, termed a "tie-down" or "termination" segment. Four segments create a section, which is the fundamental building block of tendon-driven continuum robots. A 2-section planar robot is shown in figure 2. Out of the plane, a section is basically a 2-DOF manipulator, with two pairs of opposing tendons orthogonal to each other, and it is

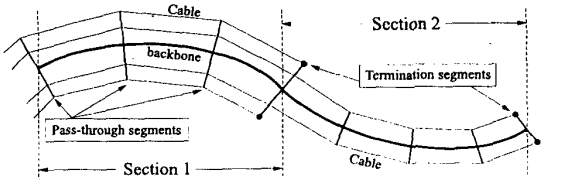

Figure 2: A 2-section planar backbone. In the plane, each section is a "1-DOF manipulator".

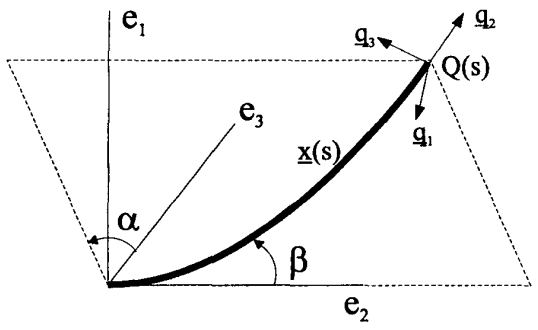

Figure 3: An illustration of how the angles α and β reflect the robot's shape.

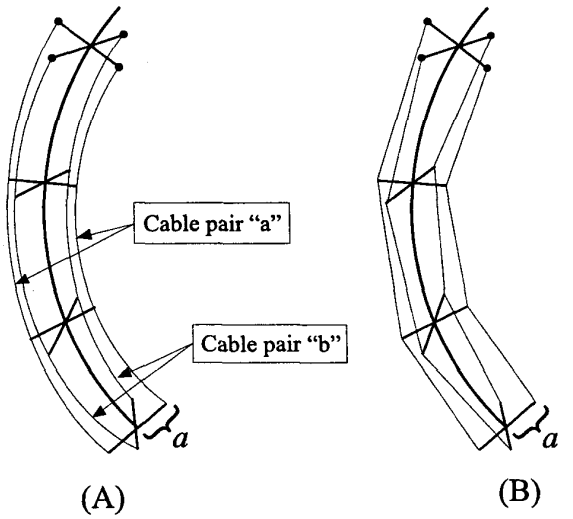

Figure 4: Figure (A) illustrates the ideal (but impractical) cable arrangement. Figure (B) shows the reality where the cables follow the backbone in straight-line segments.

necessary to understand the behavior of a section before we can comprehend the whole robot. Because cables do not drive every segment, these types of robots require the backbone to exhibit a restoring quality which will tend to straighten the backbone out, either with externally attached springs or through the nature of the backbone material.

We first ignore external parameters such as gravity, and assume that the backbone consists of a homogenous, symmetric rod (or beam) which tends to spring back to a straight line. The rod is not allowed to twist or contract or extend, and when bent, bends only in a plane perpendicular to some vector $\underline{k}$. We align one end of the rod so it lies on the $\underline{e}_2$ axis of the elementary $\{\underline{e}_1, \underline{e}_2, \underline{e}_3\}$ basis, and attach it firmly to the origin. Thus we may create a frame Q on the end of the rod using the axis/angle description [18],

$$Q = [R_{e_2,\alpha}][R_{e_1,\beta}][R_{e_2,-\alpha}] \tag{2}$$

where $[R_{e_2,\alpha}]$ represents a rotation of α about $\underline{e}_2$.

In the absence of external disturbances and forces such as gravity, α will in general remain constant with $\beta(s)$ varying, as in figure 3. In other words, a section always operates in a plane containing e_2; angle α determines exactly which plane. (There is, of course, an alternative view in terms of Euler angles, as in [16]) Now we may move the frame along the backbone by varying $\beta(s)$. Multiplying (2) gives

$$Q(s) = \begin{bmatrix} c_\alpha^2 + s_\alpha^2 c_\beta & s_\alpha s_\beta & -c_\alpha s_\alpha (1 - c_\beta) \\ -s_\alpha s_\beta & c_\beta & -c_\alpha s_\beta \\ -c_\alpha s_\alpha (1 - c_\beta) & c_\alpha s_\beta & s_\alpha^2 + c_\alpha^2 c_\beta \end{bmatrix} \tag{3}$$

(where $c_\alpha = \cos\alpha$, etc.) which is the fundamental orientational description of a section. Later we will note that gravity may pull the robot out of the plane, and thus we must concern ourselves with $\alpha(s)$ also. By convention we take $\beta(0) = 0$. Since $\underline{q}_2(s)$ is the tangent vector to the backbone, the robot position is

$$\underline{x}(s) = \int_0^s \underline{q}_2(\sigma) d\sigma = \int_0^s \begin{bmatrix} s_\alpha s_\beta & c_\beta & c_\alpha s_\beta \end{bmatrix}^T d\sigma \tag{4}$$

which completes the basic kinematic description of the robot backbone.

Again, if we wanted to "fit" a real robot to a continuous model, we could use a simpler model than (3). However, (3) more closely represents what actually occurs when a continuum robot bends, and we will need this accuracy when analyzing how the cables behave. (For instance, (1) implies that one axis of the moving frame always exists only in the $\{e_1, e_2\}$ plane, while observations of an actual backbone disagree with this implication.)

4 Issues Related to Cables

In order to understand how the robot moves, we must address the issue of how the cables bend as a section bends. Each section has two orthogonal pairs of cables, which pass through the cable guide segments and attach at the termination segment (see figures 2 and 4). We start with the (incorrect) assumption that the distance between the cable and the backbone at any point is constant, say a distance of a (figure 4A). For convenience we align the base frame of the robot ($Q(0) = I_{3\times 3}$) so that the cables start at $\pm a\underline{q}_1(0) = [\ \pm a \quad 0 \quad 0\ ]^T$ for one pair and $\pm a\underline{q}_3(0) = [\ 0 \quad 0 \quad \pm a\ ]^T$ for the other. The choice of $+$ or $-$ depends on which cable in the pair is under consideration.

Thus, as the backbone bends, the cable pairs follow the path

$$\underline{x}_{ca} = \int_0^s \underline{q}_2(\sigma) d\sigma \pm a\underline{q}_1(s) \tag{5}$$

$$\underline{x}_{cb} = \int_0^s \underline{q}_2(\sigma)d\sigma \pm a\underline{q}_3(s).$$

Without loss of generality, we substitute $\underline{q}_1(s) = \int_0^s \frac{d}{d\sigma}\underline{q}_1(\sigma)d\sigma$, and similarly substitute for $\underline{q}_3(s)$, so that (dropping the similar expression for the second cable pair)

$$\underline{x}_{ca} = \int_0^s \left\{\underline{q}_2(\sigma) \pm a\dot{\underline{q}}_1(\sigma)\right\} d\sigma. \tag{6}$$

The expression for $\dot{\underline{q}}_1(s)$ will contain $\dot{\alpha}(s)$ and $\dot{\beta}(s)$, but $\dot{\alpha} = 0$ for robots in the absence of external forces. With this in mind, it is straightforward to see that

$$\begin{aligned} \underline{x}_{ca} &= \int_0^s \underline{q}_2(\sigma)\left\{1 \pm a\dot{\beta}\sin\alpha\right\} d\sigma \\ \underline{x}_{cb} &= \int_0^s \underline{q}_2(\sigma)\left\{1 \pm a\dot{\beta}\cos\alpha\right\} d\sigma \end{aligned} \tag{7}$$

Recalling the general form of a backbone curve, $\underline{x}(s) = \int_0^s l(\sigma)\underline{q}_2(\sigma)d\sigma$, evidently $l(\sigma) = 1 \pm a\dot{\beta}(\sigma)\sin\alpha$. From this observation we can extract the cable lengths L_{ca} and L_{cb} at any point by integrating to obtain

$$\begin{aligned} L_{ca} &= \int_0^1 1 \pm a\dot{\beta}(\sigma)\sin\alpha d\sigma = 1 \pm a\beta(1)\sin\alpha \\ L_{cb} &= \int_0^1 1 \pm a\dot{\beta}(\sigma)\cos\alpha d\sigma = 1 \pm a\beta(1)\cos\alpha \end{aligned} \tag{8}$$

and, noting that the cables have unit length when the robot is not bending, the cables change length according to

$$\begin{aligned} \Delta L_{ca} &= \pm a\beta(1)\sin\alpha \\ \Delta L_{cb} &= \pm a\beta(1)\cos\alpha. \end{aligned} \tag{9}$$

Expression (9) illustrates an important quality of the tendon-driven section: if there are sufficiently numerous segments to allow the cable to approximately follow the backbone shape, changing cable lengths directly affects the orientation of the end of the section (which may be the end-effector, or the beginning of another section). The actual path of the backbone is determined by a number of factors, most notably minimum potential energy, with orientation as either a boundary condition or a system constraint. Expression (8) also suggests (as is in fact the case) that as long as the section does not bend significantly out of plane, it will maintain its end-orientation even in the presence of external disturbances (figure 5). This is manipulator *self-motion on orientation*: For each section we fix $\beta(0)$ and control $\beta(1)$ by changing appropriate cable lengths. In between, $\beta(s)$ is essentially free to assume one of an infinite array of configurations, obeying external physical system constraints. From this, we see that these types of robots possess an interesting and useful characteristic – inherent compliance. Since the controllable quantities are orientations, actual backbone position may vary (through orientational self-motion and minimum energy principles) to conform around objects in the environment, mitigating the need for complex force or impedance control schemes. For completeness, we note that, since the change in cable length is a measurable and controllable quantity, the inverse of (9) is

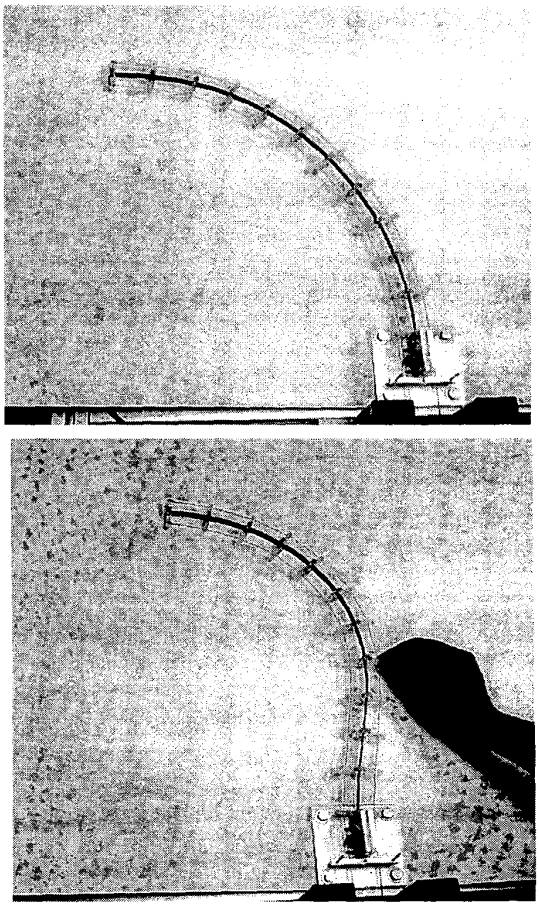

Figure 5: An 11-segment 1-DOF planar section bends into a semi-circle (top). Its end-orientation remains constant even in the presence of an external force (bottom).

$$\begin{aligned} \alpha &= \tan^{-1}\left(\frac{\Delta L_{ca}}{\Delta L_{cb}}\right) \\ \beta(1) &= \pm\frac{1}{a}\sqrt{\Delta L_{ca}{}^2 + \Delta L_{cb}{}^2} \end{aligned} \tag{10}$$

using the 4-quadrant arc-tangent.

Practically speaking, keeping the cables a constant distance from the backbone presents great difficulty; in reality we must thread the cables through guide segments (pass-through segments) and allow the cable to approximate the backbone curve similar to the perimeter of a polygon, as in fig 4B. This implies that a section should have as many pass-through segments as possible. Never-

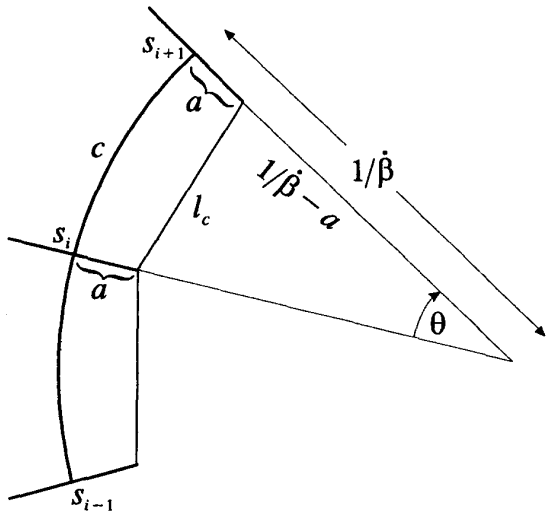

Figure 6: A close-up of two segments to illustrate how cable lengths relate to bending.

theless, while (9) predicts that the amount of cable pulled in equals the amount let out, in practice this is not quite true and it is necessary to reflect this in the mechanical design.

In order to account for the discrepancy, assume for the sake of illustration a continuum planar robot (say, $\alpha = 0$), with pass-through segments which keep the cable a distance a from the backbone. If the amount of bending is not too large, the backbone assumes a nearly circular arc between two segments (we discuss this issue later). Assuming not too much out-of-plane bending, the radius of the circle with respect to the cable is $\frac{1}{\dot{\beta}}$. With an arc length of c between segments, the arc angle is $\theta = \dot{\beta}c$ (figure 6). From this we can deduce the following relationship,

$$2\sin\left(\frac{c}{2}\dot{\beta}\right) = \frac{l_c}{\frac{1}{\dot{\beta}} - a} \tag{11}$$

where l_c is the cable length between 2 segments. Solving for l_c and simplifying yields

$$l_c = c(1 - \dot{\beta}a)\,\mathrm{sinc}\left(\frac{c}{2}\dot{\beta}\right) \tag{12}$$

where we take $\mathrm{sinc}\,(t) \triangleq \frac{\sin(t)}{t}$.

To get an estimation of true cable length for a whole section consisting of n segments, we divide the section by attaching n segments of equal length at locations s_0, s_1, $s_2, \ldots, s_n$ and replacing arc length c with $c = s_i - s_{i-1}$. We also "sample" $\dot{\beta}$ at the same locations, i.e. $\dot{\beta}(s_0)$, $\dot{\beta}(s_1)$, etc. Summing over the entire section using (12) gives

$$\sum_{i=0}^{n} l_c^{(i)} = \sum_{i=0}^{n} (s_i - s_{i-1})(1 - a\dot{\beta}(s_i))\,\mathrm{sinc}\left(\frac{(s_i - s_{i-1})}{2}\dot{\beta}(s_i)\right). \tag{13}$$

By noting that $s_0 = 0$ and $s_n = 1$, spacing the s_i's evenly yields $n \simeq 1/\Delta s$ where $\Delta s \triangleq s_i - s_{i-1}$. Taking the limit of (13) as $n \to \infty$, we obtain

$$\begin{aligned}\sum_{i=0}^{\infty} l_c^{(i)} &= \lim_{n\to\infty} \sum_{i=0}^{n} \Delta s(1 - a\dot{\beta}(s_i))\,\mathrm{sinc}\left(\frac{1}{2n}\dot{\beta}(s_i)\right) \\ &= \int_0^1 (1 - a\dot{\beta}(s))ds = 1 - a\beta(1) \end{aligned} \tag{14}$$

which is the ideal tendon length vs. bending relationship. Releasing the constraint to work in the plane, i.e. $\alpha \neq 0$, transforms (14) exactly into the ideal tendon length expression (8).

5 More on the Backbone

Given that the backbone in a section always attempts to straighten out into a line, when the end-orientation changes, the backbone will assume a minimum potential energy configuration. The constraint for minimum energy provides enough information to describe $\alpha(s)$ and $\beta(s)$ in a differential system. At a minimum, different types of potential energy stored in the robot will be "spring" energy (the tendency of the backbone to return to a straight line), inertial energy due to a load on the end of the robot, and inertial energy due to the robot's own mass. By observing how the frame $Q(s)$ changes, we may quantify the spring energy as

$$SE = \int_0^1 \frac{1}{2} w(s) \left\| \dot{Q}(s)^T \dot{Q}(s) \right\|_F^2 ds \tag{15}$$

where $w(s)$ weights the relative "bendability" of the backbone along its length, and $\|\cdot\|_F$ is the Frobenius norm, or 'F' norm. For the frame chosen in (3),

$$SE = \int_0^1 w(s) \left[2\dot{\alpha}^2(1 - \cos\beta) + \dot{\beta}^2 \right] ds. \tag{16}$$

In general we may model the potential energy from gravity as

$$PE = \int_0^1 gh(\alpha(s), \beta(s))ds \tag{17}$$

where g is the gravitational acceleration, and $h(\alpha(s), \beta(s))$ contains quantities of mass times height. For instance, assuming gravity acts in the direction of $\underline{e}_1$, a mass m_l on the end of the backbone gives $PE = g\int_0^1 m_l \sin(\alpha)\sin(\beta)ds$. By summing the energies in (16) and (17) we can obtain a cost function to be minimized by utilizing the Lagrangian,

$$\mathcal{L} = w(s)\left[\dot{\alpha}^2(1 - \cos\beta) + \frac{1}{2}\dot{\beta}^2\right] + gh(\alpha(s), \beta(s)). \tag{18}$$

According to the rules of variational calculus [17] we may then set

$$\frac{\partial \mathcal{L}}{\partial \alpha} - \frac{d}{ds}\frac{\partial \mathcal{L}}{\partial \dot{\alpha}} = 0\,;\; \frac{\partial \mathcal{L}}{\partial \beta} - \frac{d}{ds}\frac{\partial \mathcal{L}}{\partial \dot{\beta}} = 0 \tag{19}$$

which becomes the differential system

$$\begin{aligned} \ddot{\alpha}(1-\cos\beta) &= \frac{g}{2w}\frac{\partial h}{\partial \alpha} - \frac{\dot{w}}{w}\dot{\alpha}(1-\cos\beta) - \dot{\alpha}\dot{\beta}(\sin\beta) \\ \ddot{\beta} &= \frac{g}{w}\frac{\partial h}{\partial \beta} - \frac{\dot{w}}{w}\dot{\beta} + \dot{\alpha}^2(\sin\beta) \end{aligned} \quad (20)$$

where $w(s)$ is a nonzero, pre-determined function independent of α and β. The initial and final conditions on (20) are

$$\begin{aligned} \beta(0) &= 0 \qquad \beta(1) = \frac{1}{a}\sqrt{\Delta L_{ca}{}^2 + \Delta L_{cb}{}^2} \quad (21) \\ \alpha(0) &= \tan^{-1}\left(\frac{\Delta L_{ca}}{\Delta L_{cb}}\right) \qquad \dot{\alpha}(0) = 0 \end{aligned}$$

which is to say, we expect $\alpha(s)$ to remain constant, with the final condition on $\beta(s)$ determined by the desired orientation of the backbone section. Upon close inspection, the system in (20) contains a singularity at $\beta = n\pi$, $n = 0, 1, 2...$, which cannot be avoided because $\beta(0) = 0$. Since the study of non-linear ODE's with singularities is a subject too lengthy to cover here, we will simply note some of the qualitative features of (20).

First, we note that in the absence of gravity ($g = 0$), the expression involving $\ddot{\alpha}$ contains no forcing or restoring terms, i.e. terms independent of $\dot{\alpha}$ and $\ddot{\alpha}$. Thus, we can probably expect α to remain constant over the given backbone section because $\dot{\alpha}(0) = 0$. (This is borne out by numerical computations and observation, but is by no means analytically clear due to the singularity.) Similarly, if $\dot{\alpha}$ is relatively small (or zero), $\dot{\alpha}^2(\sin\beta)$ will be negligible, and the calculation for $\beta(s)$ decouples from terms involving α. Further, in practical laboratory devices we find that it is simpler to construct devices of constant "bendability", thus $\dot{w} = 0$ for a section. Gathering these observations together, we may qualitatively observe that, if the ratio $\frac{g}{w}$ is small enough, then $\dot{\alpha}$ will remain small, rendering $\dot{\alpha}^2$ negligible. With $\dot{w} = 0$, the calculation of $\beta(s)$ greatly simplifies, since

$$\ddot{\beta} = (small)\cdot\frac{\partial h}{\partial \beta} - 0\cdot\dot{\beta} + (verysmall)\cdot\sin\beta \quad (22)$$

so, in the plane or with total absence of gravity, $\ddot{\beta} \cong 0$ implying $\beta(s) = \mu_1 s$ (where $\mu_1 = \frac{1}{a}\sqrt{\Delta L_{ca}{}^2 + \Delta L_{cb}{}^2}$); this is the expression for a circle of constant radius $\frac{1}{\mu_1}$, as expected.

In general, we can state the following rather intuitive design rules: a manipulator section should be stiff enough so that the quantity $\frac{g}{w}\nabla h(\alpha(s), \beta(s))$ remains acceptably small, and each section's backbone should preferably be constructed of a homogeneous material which does not prefer to bend at any particular point.

6 Attaching Multiple Sections Together

Having discussed the properties of a single 2-DOF section of backbone, we naturally desire to progress to a discussion of the entire robot, consisting of many such sections attached in series. There are several questions to consider when building the robot, including whether to maintain the tendons for a distal section at a non-zero distance from the backbone of a proximal section. Also, the designer must consider how many segments each section should consist of in order to strike a balance between minimizing friction on the cables and keeping their shape close to that of the backbone. Essentially, we can see the overall kinematic structure by multiplying several section frames together, from (2),

$$\begin{aligned} Q(s) = {} & [R_{e_2,\alpha_1}][R_{e_1,\beta_1}][R_{e_2,\alpha_2-\alpha_1}][R_{e_1,\beta_2}][R_{e_2,\alpha_3-\alpha_2}] \\ & \cdots[R_{e_2,\alpha_n-\alpha_{n-1}}][R_{e_1,\beta_n}][R_{e_2,-\alpha_n}] \end{aligned} \quad (23)$$

where we have attached n sections together. The position $\underline{x}(s) = \int_0^s \underline{q}_2(\sigma)d\sigma$ as before, for a non-extensible backbone. Now the position and orientation are functions of $\alpha_i(s)$ and $\beta_i(s)$ for $i = 1..n$, which must be computed for each section. These functions have a special form illustrated in (24). Setting the robot's total backbone length to unity, we may divide the robot into n sections in a similar fashion to dividing a section into segments. We sample the total arc length at points $s_0, s_1, s_2, ..., s_n$, note that $s_0 = 0$, and define the "ith" section as that where $s \in [s_{i-1}, s_i]$. Then, functions $\alpha_i(s)$ and $\beta_i(s)$ have the general form

$$\alpha_i(s) = \left\{ \begin{array}{ll} 0 & s < s_{i-1} \\ \alpha(s) & s_{i-1} \le s \le s_i \\ \alpha(s_i) & s > s_i \end{array} \right\} \quad (24)$$

and similarly for $\beta_i(s)$. Note that these functions vary only on $s \in [s_{i-1}, s_i]$, and remain constant before and after that interval. The variable portions, $\alpha(s)$ and $\beta(s)$, obey the rules for a section from (20); only a slight modification must be made to the initial conditions so that

$$\beta_i(s_{i-1}) = \beta_{i-1}(s_{i-1}). \quad (25)$$

In general, the complete description in (23) is cumbersome and unwieldy, though quite similar in that respect to traditional rigid-link robots. The simplest place to begin analyzing the behavior of multiple section robots is again in the plane. There we discuss such issues how to map the desired robot shape back to a finite number of actuators [3]. We can employ physical, kinematic properties explored in this work to make intelligent choices regarding modes for modal shape decomposition; see [9].

7 Conclusions and Further Work

In this paper we begin to explore the basics of cable-driven continuum robots. We lay the mathematical foun-

dations with the assignment of basic kinematic necessities such as the coordinate frame, then proceed with a discussion of how changing cable lengths varies the shape of the robot backbone. We briefly touch on the problem of connecting multiple sections together to form a higher degree-of-freedom device.

While cable-driven backbone robots do posses several drawbacks, they appear to offer an overall viable (and less expensive) alternative to simply building high-degree-of-freedom rigid-link robots. Additionally, they exhibit properties such as inherent compliance and a high degree of scalability which may make them quite useful in cluttered and crowded environments. Current and future work centers on characterizing and exploiting these properties, obtaining better kinematic and dynamic models, formulating appropriate motion control laws, and constructing experimental prototypes. Also, because of inevitable unmodeled effects and external forces, no kinematic description will be perfect and work must be done to investigate direct-sensing options (perhaps vision) for fusing observations of where the robot is with where it is expected to be.

The authors gratefully acknowledge the support of NSF grant CMS-9796328, DOE contract DE-FG07-97ER1483, and NSF/EPSCoR grant EPS-9630167. Thanks to Brian Bunnell and Michael Hannan for help constructing the robot prototypes.

References

[1] S. Hirose, *Biologically Inspired Robots*. Oxford University Press, 1993

[2] I.D. Walker and M.W. Hannan, "A Novel Elephant's Trunk Robot", IEEE/ASME Intl. Conf. on Advanced Intelligent Mechatronics, Atlanta, GA, Sept. 1999, pp. 410-415

[3] I. Gravagne and I.D. Walker, "Kinematic Transformations for Remotely-Actuated Planar Continuum Robots," IEEE Int'l Conf. on Robotics and Automation (ICRA), San Fransisco, May 2000.

[4] GreyPilgrim company, http://www.greypilgrim.com

[5] R. Cieslak and A. Morecki, "Elephant Trunk Type Elastic Manipulator - a Tool for Bulk and Liquid Materials Transportation," Robotica, 1999, Vol. 17 pp. 11-16

[6] H. Mochiyama and H. Kobayashi, "The Shape Jacobian of a Manipulator with Hyper Degrees of Freedom," Proceedings 1999 IEEE Int'l Conf. on Robotics and Automation (ICRA), Detroit MI, May 1999, pp. 2837-2842

[7] H. Mochiyama and H. Kobayashi, "Shape Correspondence between a Spatial Curve and a Manipulator with Hyper Degrees of Freedom," Proceedings 1998 IEEE/RSJ Int'l Conf. on Intelligent Robots and Systems, Victoria, Canada, October 1998, pp. 161-166

[8] H. Mochiyama, E. Shimemura and H. Kobayashi, "Direct Kinematics of Manipulators with Hyper Degrees of Freedom and Serret-Frenet Formula," Proceedings 1998 IEEE Int. Conf. Robotics and Automation, Leuven, Belgium, May 1998, pp. 1653-1658

[9] G.S. Chirikjian and J.W. Burdick, "A Modal Approach to Hyper-Redundant Manipulator Kinematics," IEEE Transactions on Robotics and Automation, vol. 10, no. 3, June 1994, pp. 343-353

[10] G.S. Chirikjian and J.W. Burdick, "Kinematically Optimal Hyper-Redundant Manipulator Configurations," IEEE Trans. Robotics and Automation, vol. 11, no. 6, Dec 1995, pp. 794-80

[11] G.S. Chirikjian, "A General Numerical Method for Hyper-Redundant Manipulator Inverse Kinematics," Proc. IEEE Int. Conf. Robotics and Automation, Atlanta GA, May 1993, pp. 107-112

[12] G.S. Chirikjian and J.W. Burdick, "Kinematically Optimal Hyper-Redundant Manipulator Configurations," Proc. IEEE Int. Conf. Robotics and Automation, Nice, France, May 1992, pp. 415-420

[13] G.S. Chirikjian and J.W. Burdick, "An Obstacle Avoidance Algorithm for Hyper-Redundant Manipulators," Proc. IEEE Int. Conf. Robotics and Automation, Cincinatti, OH, May 1990, pp. 625-631

[14] G.S. Chirikjian, "Theory and Applications of Hyper-Redundant Robotic Manipulators," Ph.D. thesis, Dept. of Applied Mechanics, California Institute of Technology, June, 1992

[15] G. Robinson and J.B.C. Davies, "Continuum Robots - A State of the Art," Proc. IEEE Int. Conf. Robotics and Automation, Detroit, MI, May 1999, pp. 2849-2854

[16] K. Suzumori, S. Ilkura, and H. Tanaka, "Development of Flexible Microactuator and Its Applications to Robotic Mechanisms," Proc IEEE Int. Conf. Robotics and Automation, Sacramento, CA, April 1991, pp. 1622-1627

[17] Robert Weinstock, *Calculus of Variations with Applications for Physics and Engineering*, Dover Pulications, NY, 1974

[18] M.W. Spong and M. Vidyasagar, *Robot Dynamics and Control*, John Wiley & Sons, 1989